Electronic Supplementary Material (ESI) for Journal of Materials Chemistry A.

Electronic Supplementary Information (ESI) for:

Addressing the Stability Challenges of TiO_x-Based Passivating Contacts for High-Efficiency c-Si Solar Cells

Mohamed M. Shehata[a,b],* Thien N.Truong[a], Gabriel Bartholazzi [a], Daniel H. Macdonald [a], and Lachlan E. Black [a] *

[a]School of Engineering, The Australian National University, Canberra, ACT 2600, Australia
[b]Department of Physics, Faculty of Science, Minia University, El Minya City, 61519 Egypt

*mohamed.ismael@anu.edu.au; mohamed.shehata@mu.edu.eg and lachlan.black@anu.edu.au

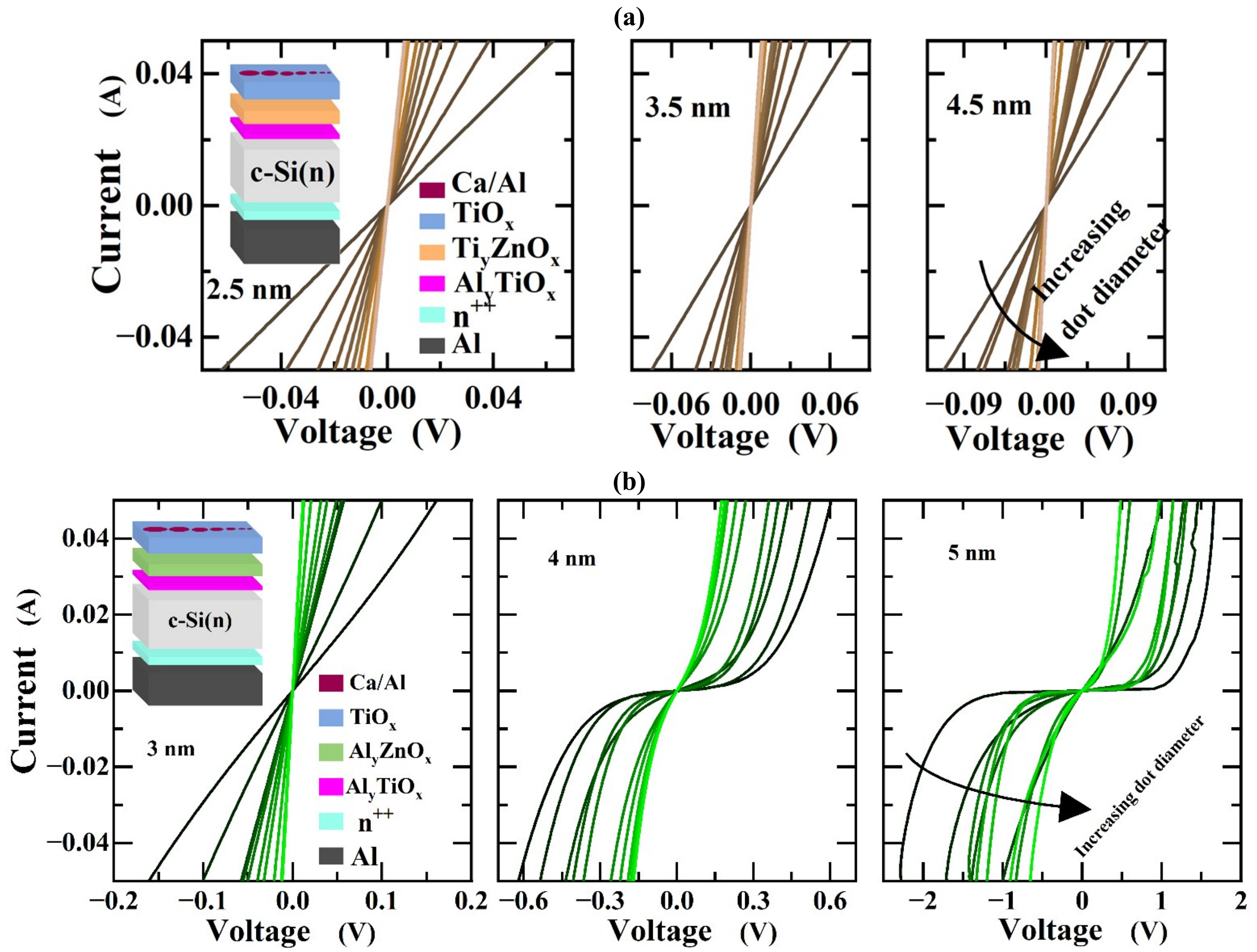

Figure S1 Dark current–voltage curves for Cox–Strack structures featuring **(a)** $Al_yTiO_x/Ti_yZnO_x/TiO_x$ and **(b)** $Al_yTiO_x/Al_yZnO_x/TiO_x$ stacks as a function of total stack thickness.

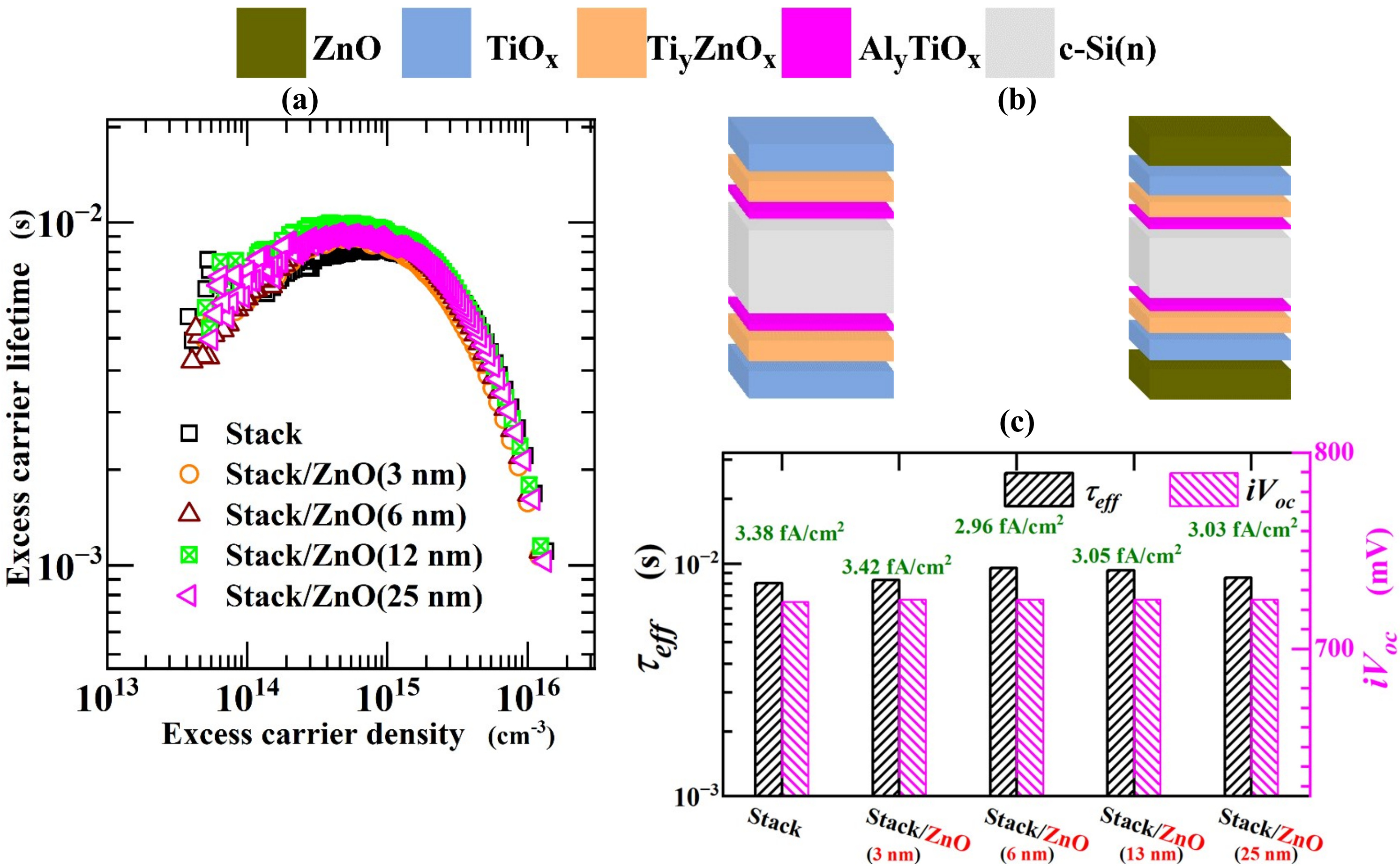

Figure S2 (a) Excess carrier lifetime as a function of excess carrier density for Si lifetime samples passivated by the $Al_yTiO_x/Ti_yZnO_x/TiO_x$ stack capped by different thicknesses of ZnO (ranging from 0 nm to 25 nm). **(b)** Corresponding schematic sample structure for symmetrically passivated lifetime samples with the stack and stack/ZnO structures. **(c)** Variation of τ_{eff} (effective carrier lifetime) and iV_{oc} (implied open-circuit voltage) for these different configurations, with the J_0 (surface recombination current density prefactor) values provided in fA/cm^2.

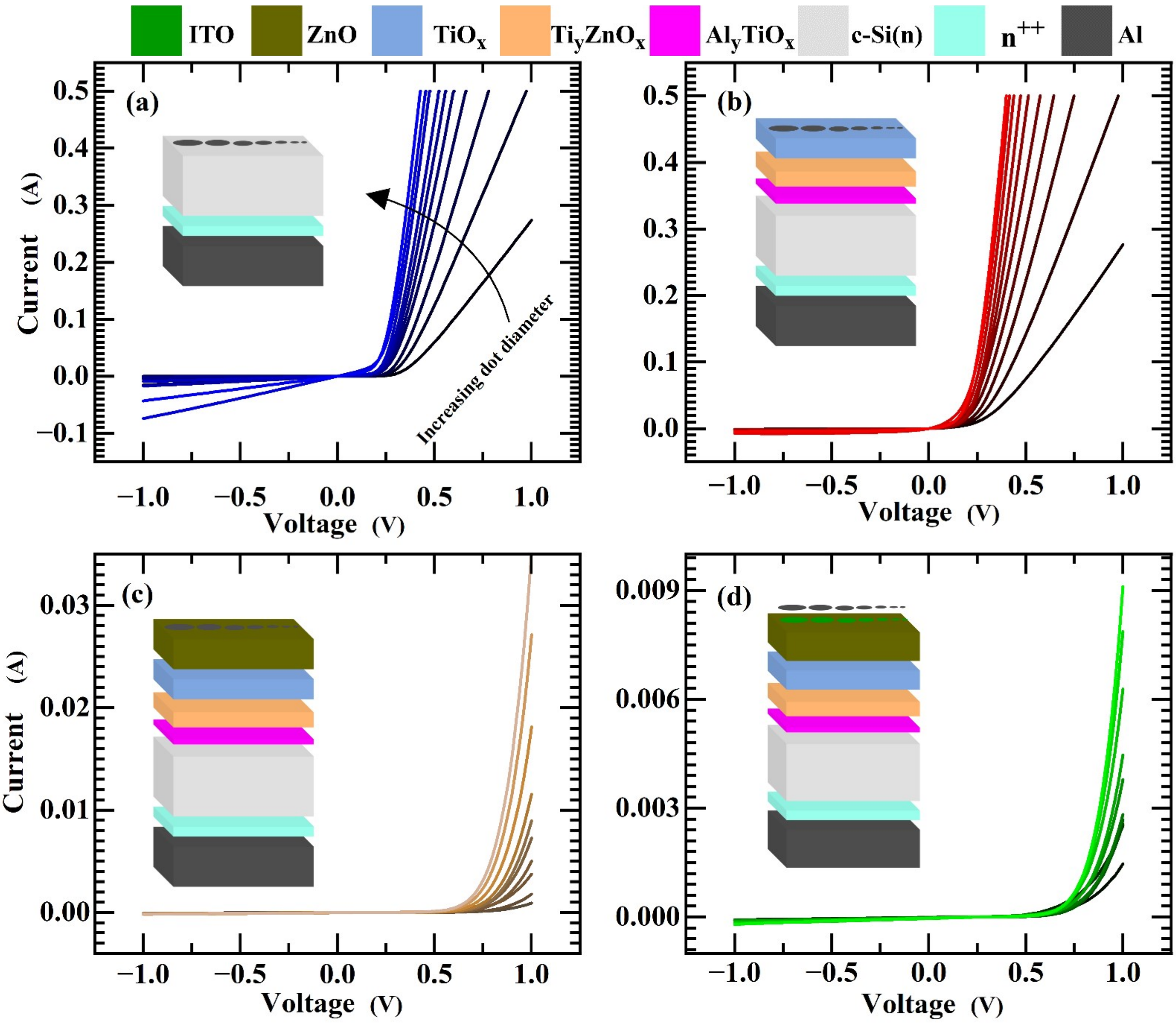

Figure S3 (a,b,c,d) Dark current–voltage curves for Cox–Strack structures with the following configurations: Si/Al, Si/stack/Al, Si/stack/ZnO/Al, and Si/stack/ZnO/ITO/Al, respectively. The "stack" structure in all configurations consists of $Al_yTiO_x/Ti_yZnO_x/TiO_x$.

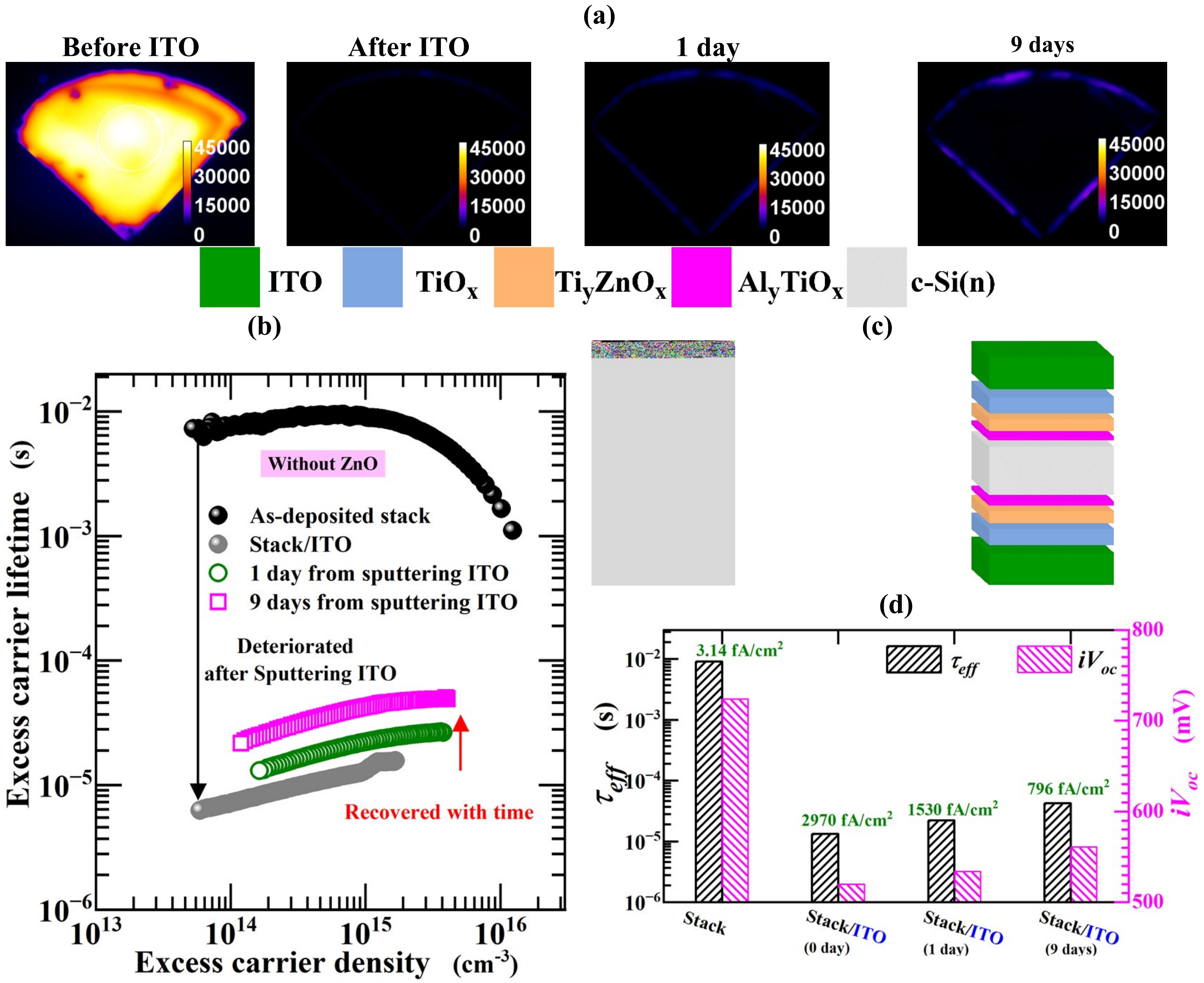

Figure S4 (a) Photoluminescence intensity imaging and **(b)** excess carrier concentration vs excess carrier density for lifetime test structures passivated by the $Al_yTiO_x/Ti_yZnO_x/TiO_x$ stack before and after sputtering ITO. The samples sputtered with ITO were subsequently measured after 1 day and again after 9 days to assess their temporal behaviour. **(c)** Schematic diagram of the stack and stack/ITO structures. **(d)** Corresponding variation of τ_{eff} (effective carrier lifetime) and iV_{oc} (implied open-circuit voltage), with the J_0 (surface recombination current density prefactor) values provided in fA/cm^2.

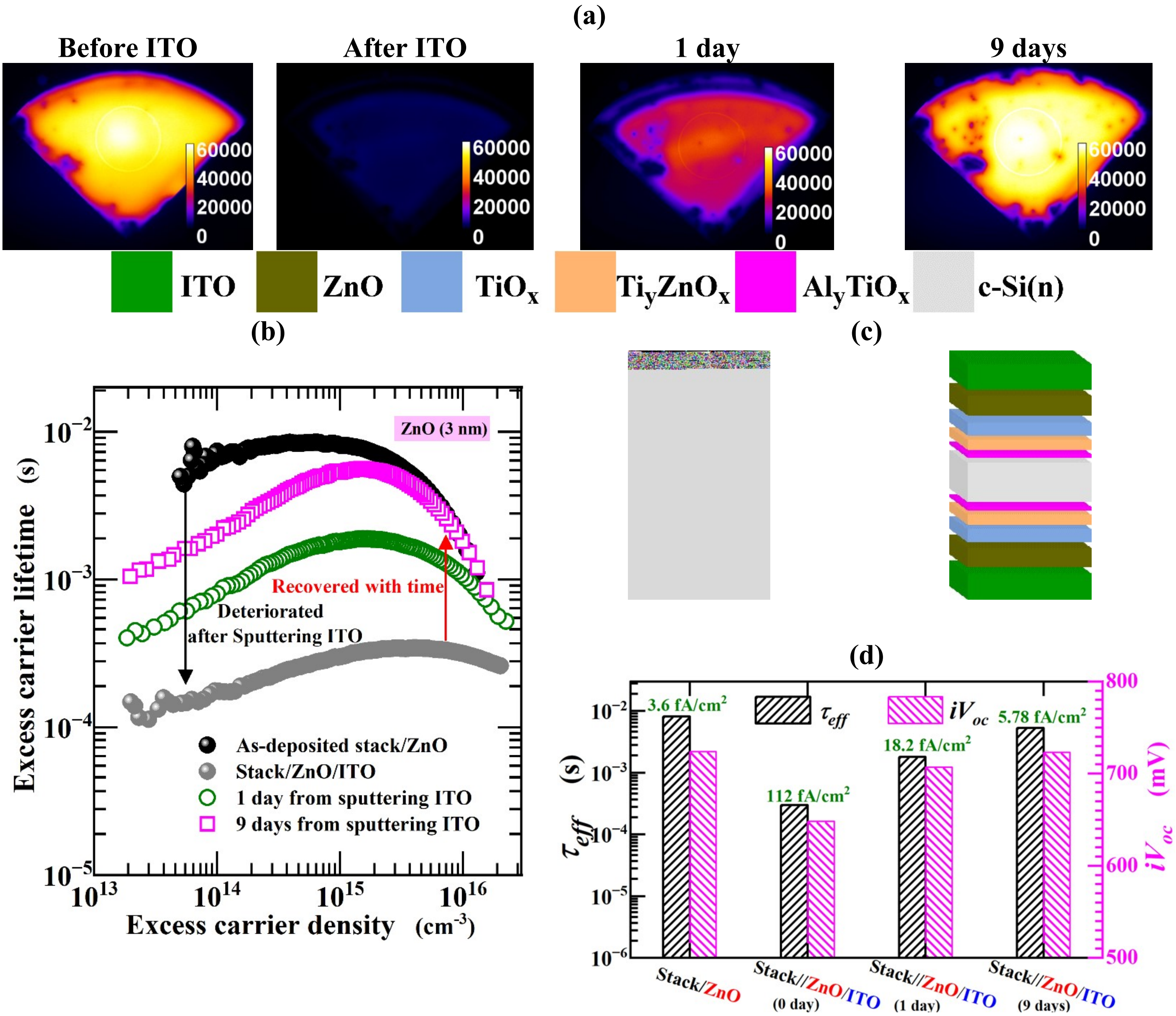

Figure S5 (a) Photoluminescence intensity imaging and **(b)** excess carrier lifetime vs excess carrier density for lifetime test structures passivated by the $Al_yTiO_x/Ti_yZnO_x/TiO_x$ stack capped by 3 nm of ZnO before and after sputtering ITO. The samples sputtered with ITO were subsequently measured after 1 day and again after 9 days to assess their temporal behaviour. **(c)** Schematic diagram of the stack and stack/ITO structures. **(d)** Corresponding variation of τ_{eff} (effective carrier lifetime) and iV_{oc} (implied open-circuit voltage), with the J_0 (surface recombination current density prefactor) values provided in fA/cm^2.

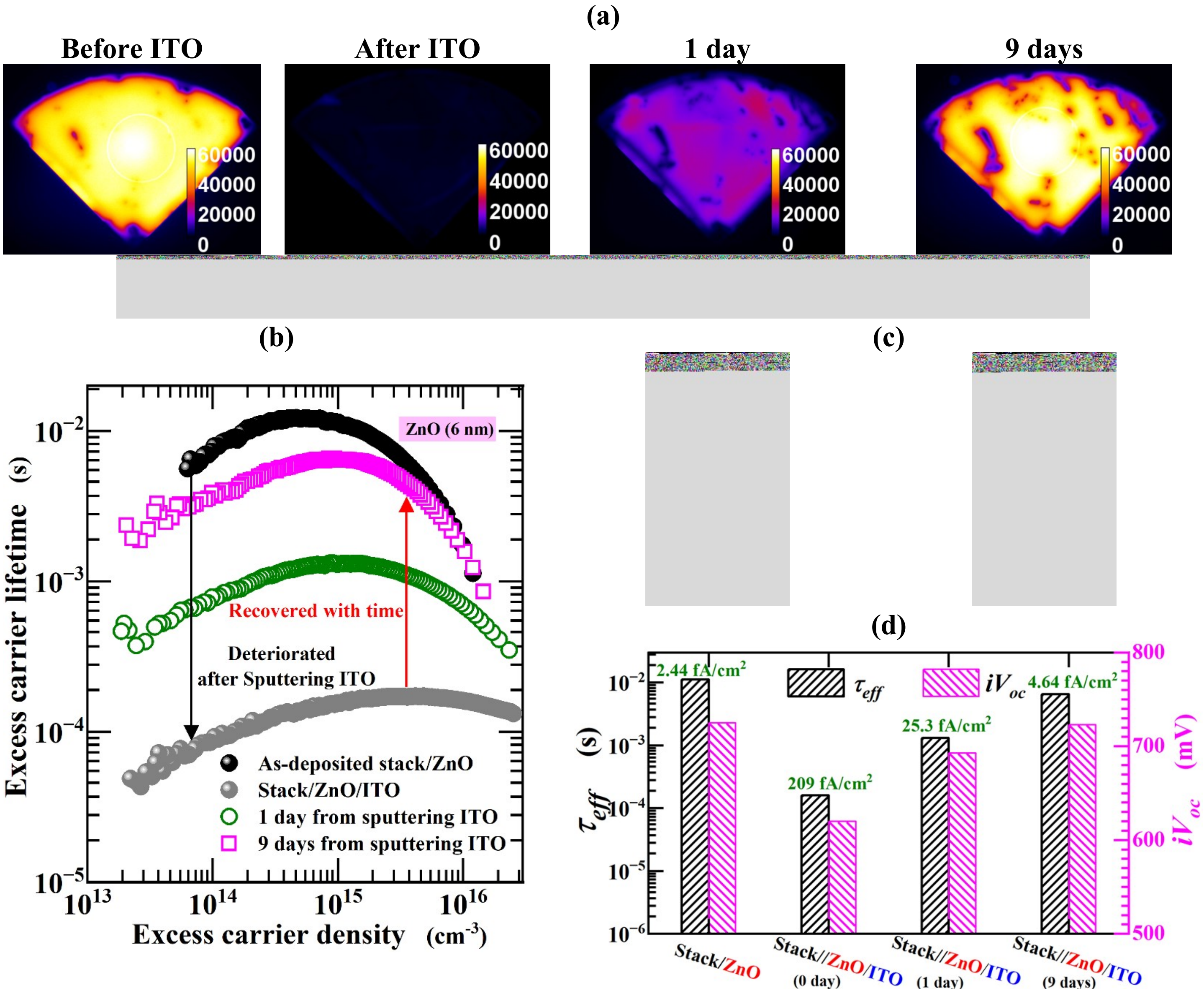

Figure S6 (a) Photoluminescence intensity imaging and **(b)** excess carrier lifetime vs excess carrier density for lifetime test structures passivated by the $Al_yTiO_x/Ti_yZnO_x/TiO_x$ stack capped by 6 nm of ZnO before and after sputtering ITO. The samples sputtered with ITO were subsequently measured after 1 day and again after 9 days to assess their temporal behaviour. **(c)** Schematic diagram of the stack and stack/ITO structures. **(d)** Corresponding variation of τ_{eff} (effective carrier lifetime) and iV_{oc} (implied open-circuit voltage), with the J_0 (surface recombination current density prefactor) values provided in fA/cm^2.

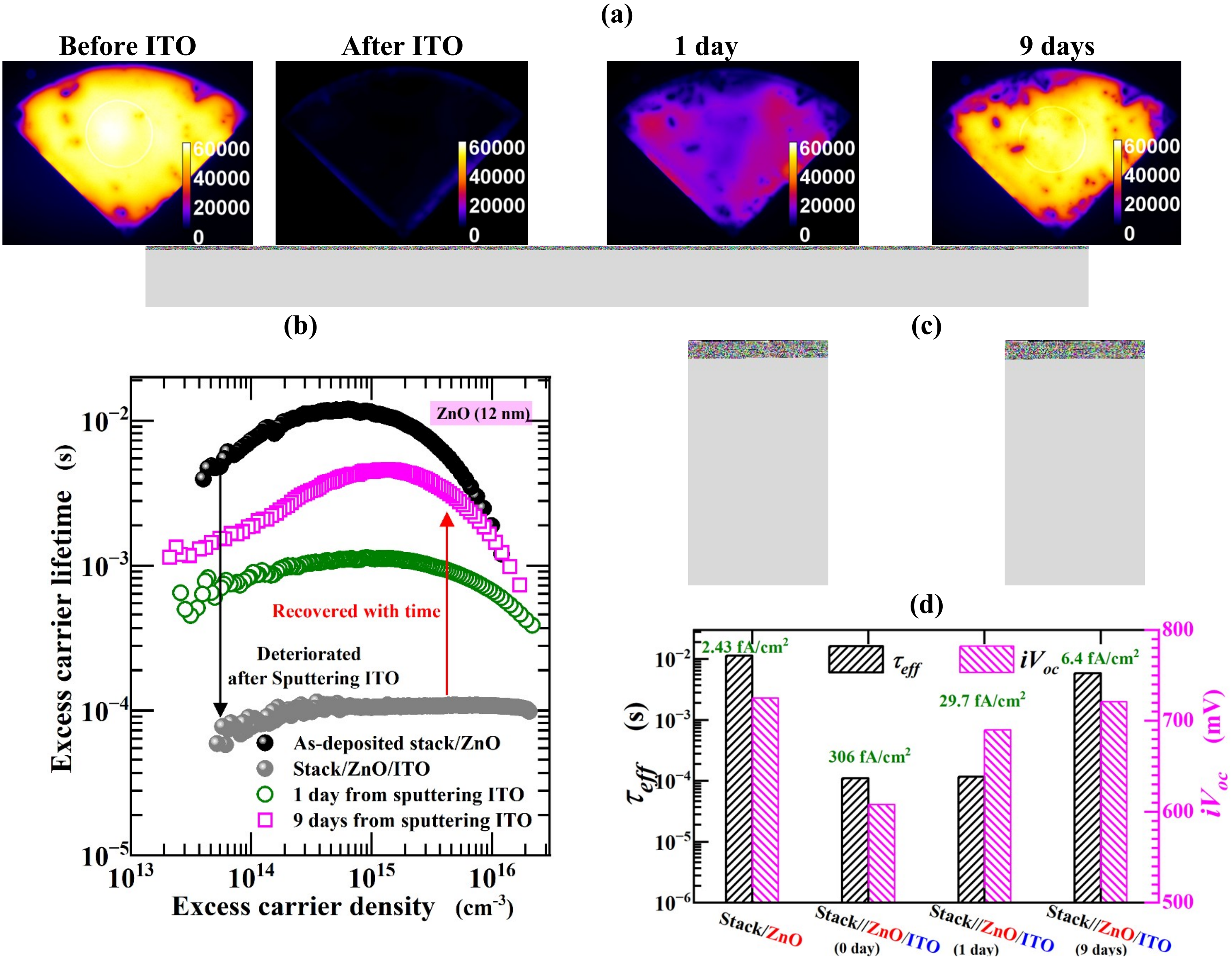

Figure S7 (a) Photoluminescence intensity imaging and **(b)** excess carrier lifetime vs excess carrier density for lifetime test structures passivated by the $Al_yTiO_x/Ti_yZnO_x/TiO_x$ stack capped by 12 nm of ZnO before and after sputtering ITO. The samples sputtered with ITO were subsequently measured after 1 day and again after 9 days to assess their temporal behaviour. **(c)** Schematic diagram of the stack and stack/ITO structures. **(d)** Corresponding variation of τ_{eff} (effective carrier lifetime) and iV_{oc} (implied open-circuit voltage), with the J_0 (surface recombination current density prefactor) values provided in fA/cm^2.

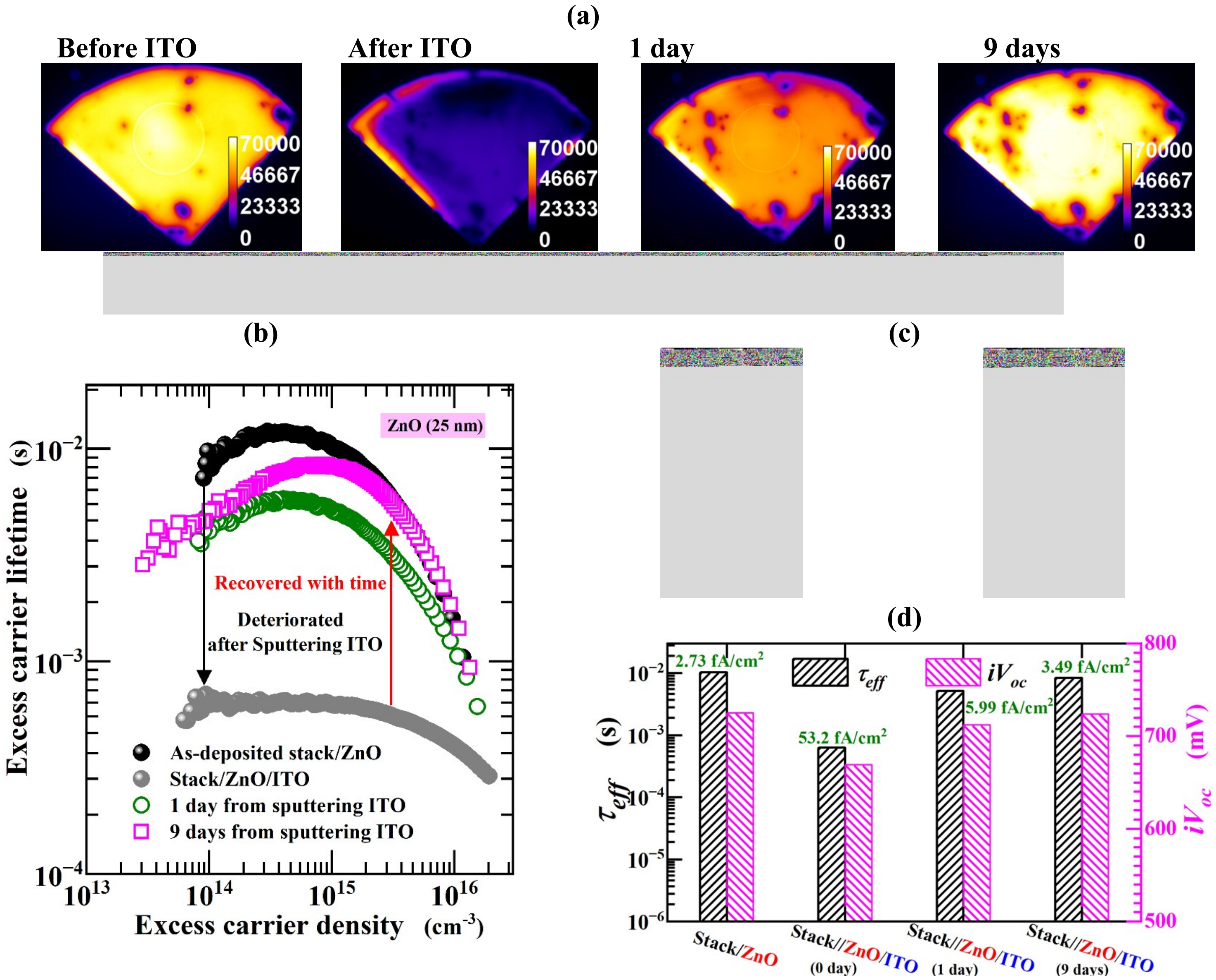

Figure S8 (a) Photoluminescence intensity imaging and **(b)** excess carrier lifetime vs excess carrier density for lifetime test structures passivated by the $Al_yTiO_x/Ti_yZnO_x/TiO_x$ stack capped by 25 nm of ZnO before and after sputtering ITO. The samples sputtered with ITO were subsequently measured after 1 day and again after 9 days to assess their temporal behaviour. **(c)** Schematic diagram of the stack and stack/ITO structures. **(d)** Corresponding variation of τ_{eff} (effective carrier lifetime) and iV_{oc} (implied open-circuit voltage), with the J_0 (surface recombination current density prefactor) values provided in fA/cm^2.

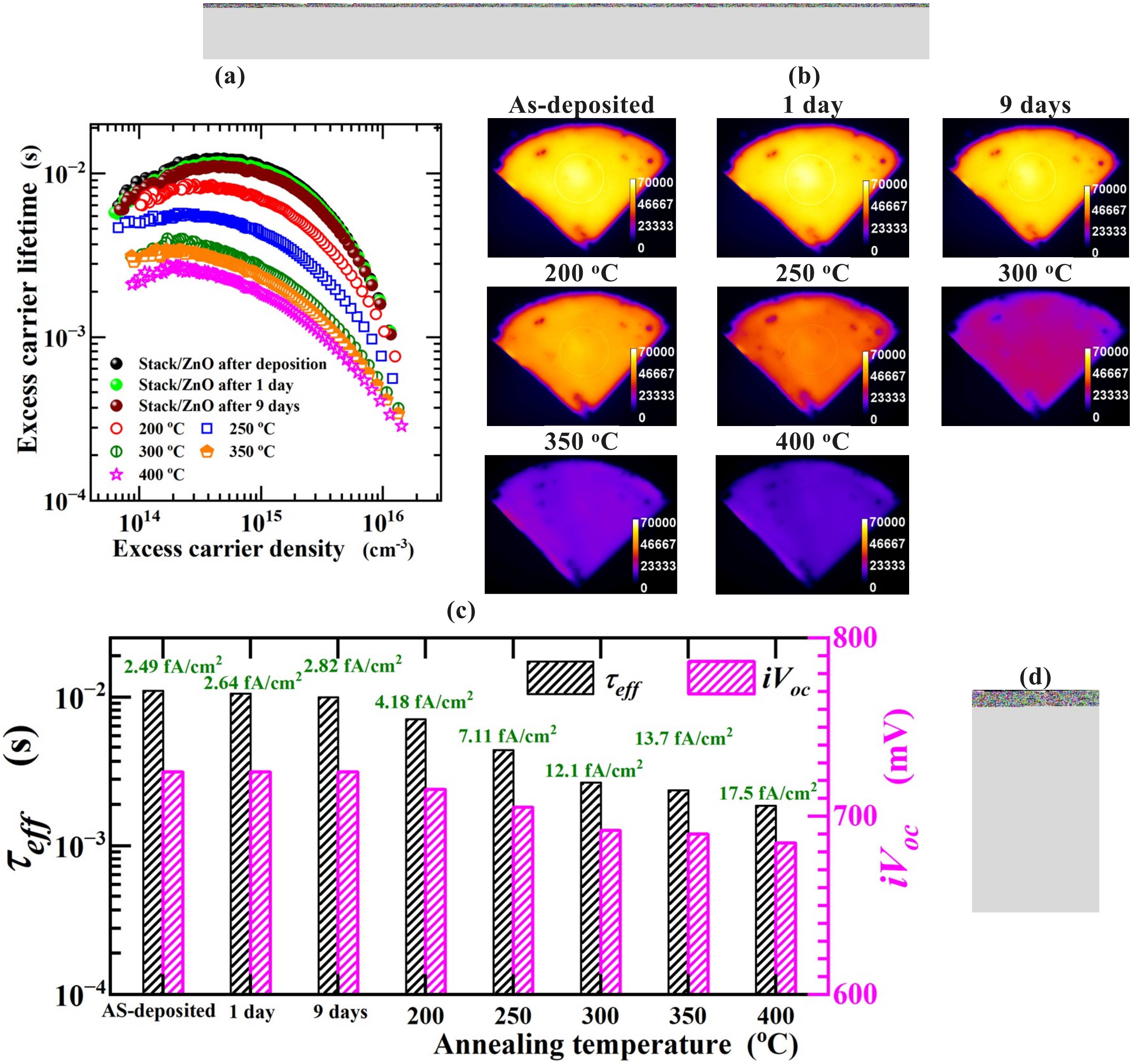

Figure S9 (a) Excess carrier lifetime vs excess carrier density for lifetime test structures passivated by the $Al_yTiO_x/Ti_yZnO_x/TiO_x$ stack capped by ZnO, as a function of annealing temperature. **(b)** Corresponding photoluminescence (PL) intensity images. **(c)** Corresponding variation of τ_{eff} (effective carrier lifetime) and iV_{oc} (implied open-circuit voltage), with the J_0 (surface recombination current density prefactor) values provided in fA/cm^2. **(d)** Schematic diagram of the stack/ZnO sample structure.

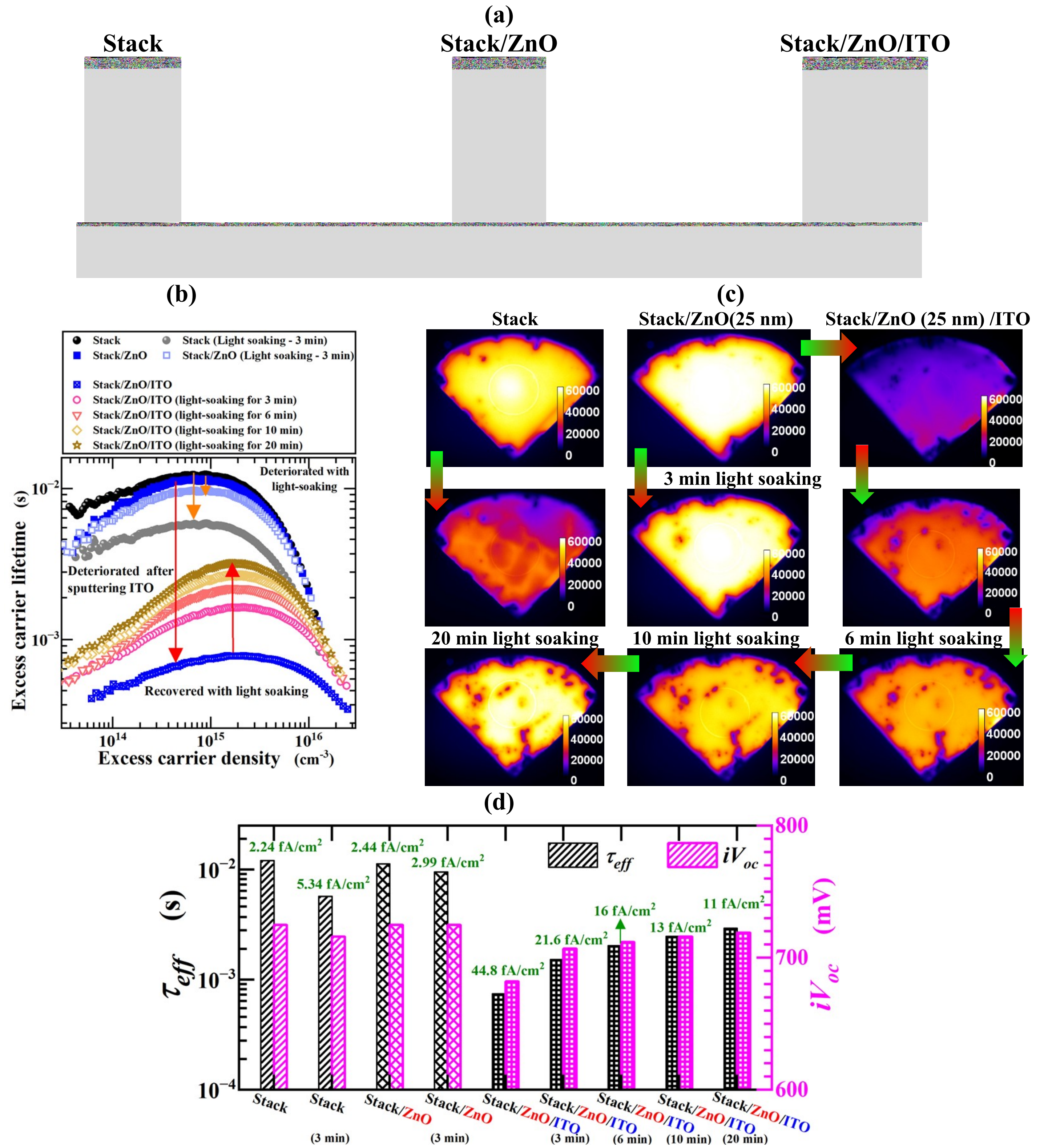

Figure S10 (a) Schematic diagrams of the stack, stack/ZnO, and stack/ZnO/ITO sample structures. **(b)** Excess carrier lifetime vs excess carrier density for lifetime test structures passivated by the $Al_yTiO_x/Ti_yZnO_x/TiO_x$ stack, either alone or capped by ZnO or ZnO/ITO, before and after light soaking. **(c)** Corresponding photoluminescence (PL) intensity imaging before and after light soaking for these samples. **(d)** Corresponding variation of τ_{eff} (effective carrier lifetime) and iV_{oc} (implied open-circuit voltage) for these samples, with the J_0 (surface recombination current density prefactor) values provided in fA/cm^2.

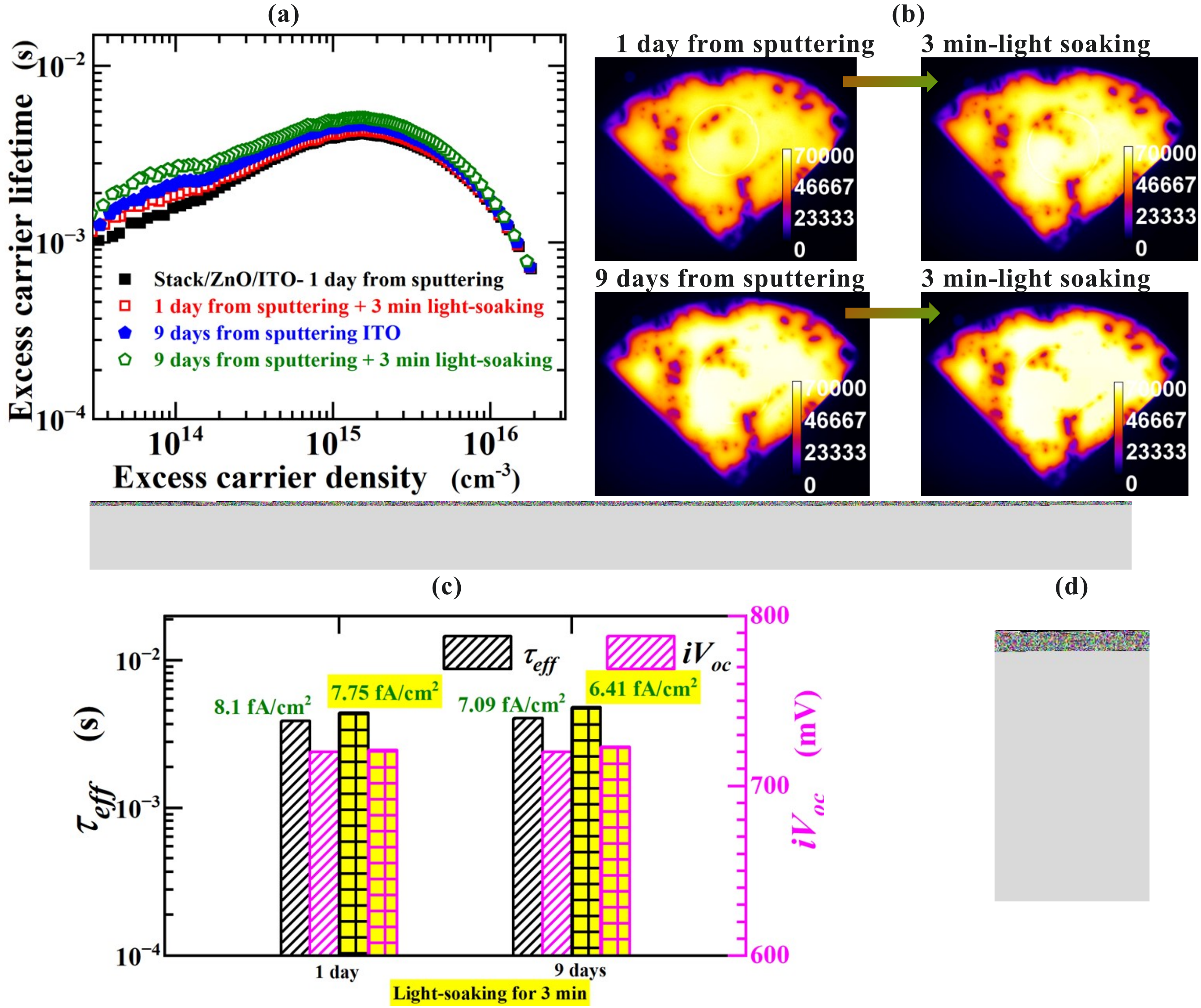

Figure S11(a) Excess carrier lifetime vs excess carrier density for the stack/ZnO/ITO lifetime test structure of Figure S10, before and after light soaking at 1 day and 9 days after sputtering of the ITO. **(b)** Corresponding photoluminescence (PL) intensity imaging before and after light soaking for these samples. **(d)** Corresponding variation of τ_{eff} (effective carrier lifetime) and iV_{oc} (implied open-circuit voltage), with the J_0 (surface recombination current density prefactor) values provided in fA/cm^2. **(d)** Schematic diagram of the stack/ZnO/ITO sample structure.

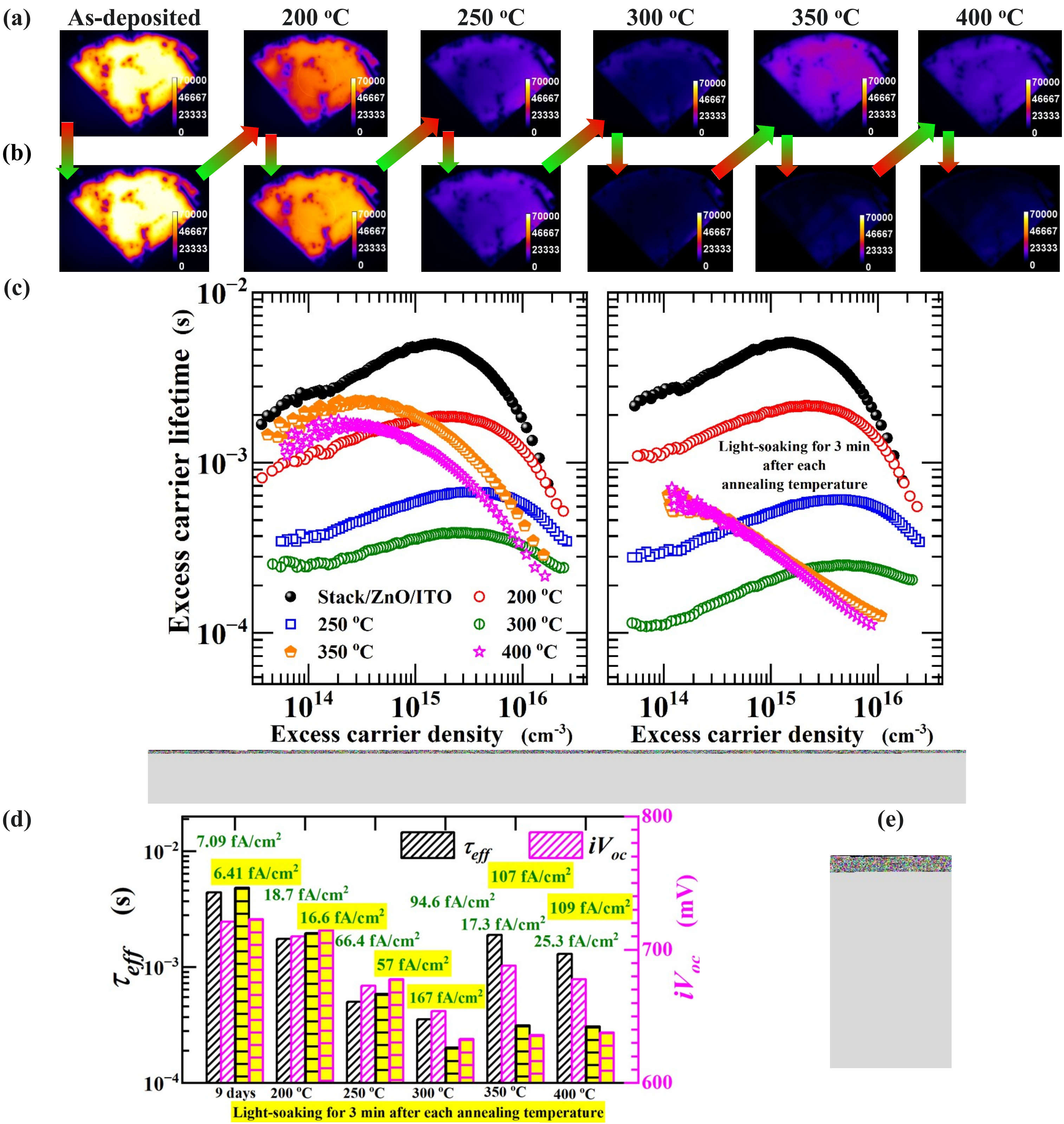

Figure S12 Photoluminescence (PL) intensity imaging for the stack/ZnO/ITO lifetime test structure of Figure S11, **(a)** after annealing at a range of increasing temperatures in N_2 for 3 minutes per anneal, and **(b)** after a 3-minute light soaking treatment subsequent to each anneal step. **(c)** Corresponding excess carrier lifetime vs excess carrier density as a function of annealing temperature, shown on the left after each annealing step, and on the right after light soaking following each annealing step. **(d)** Corresponding variation of τ_{eff} (effective carrier lifetime) and iV_{oc} (implied open-circuit voltage), with the J_0 (surface recombination current density prefactor) values provided in fA/cm^2. **(e)** Schematic diagram of the stack/ZnO/ITO sample structure.

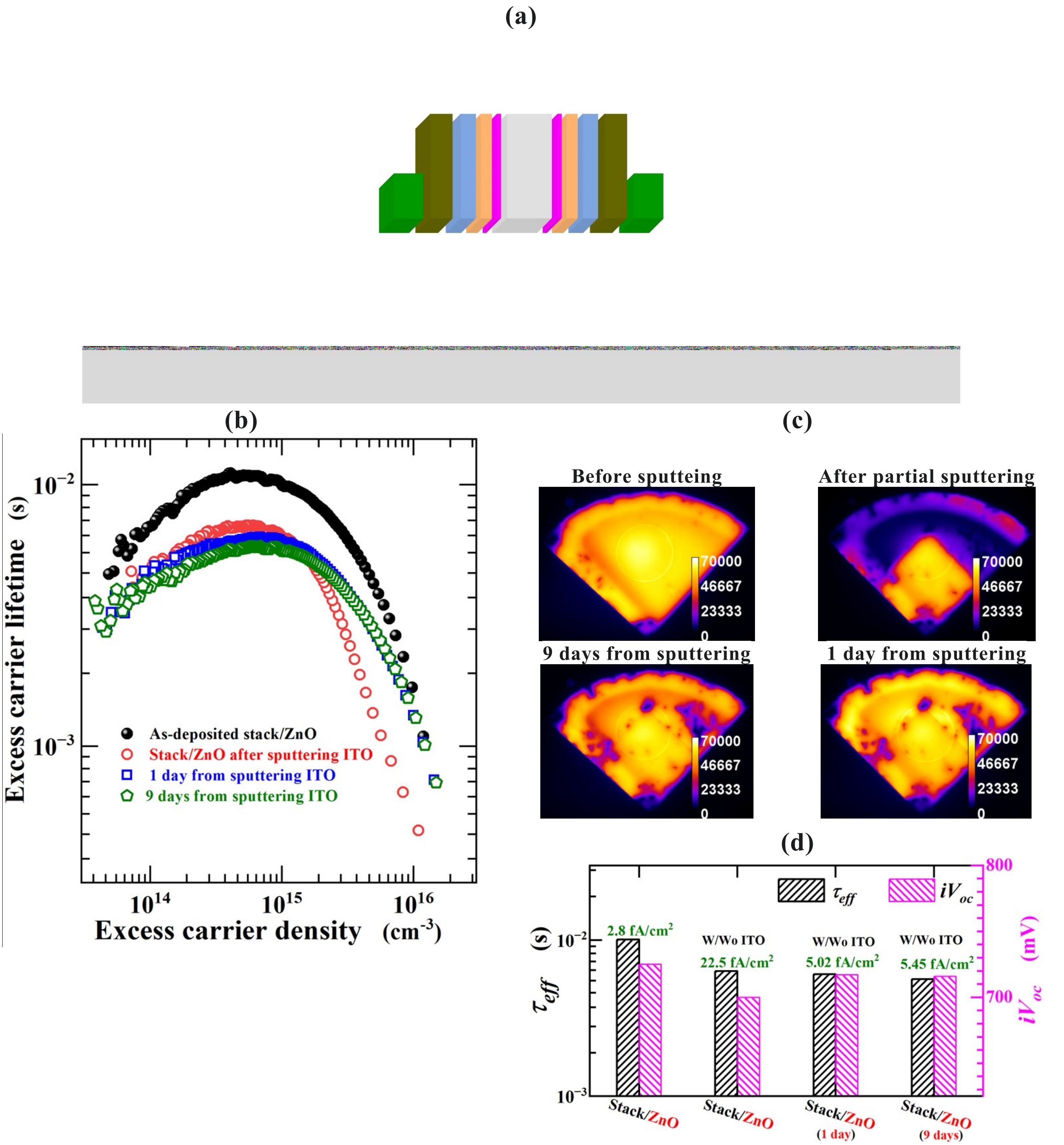

Figure S13 (a) Schematic diagram of the stack/ZnO structure with partial coverage of ITO. **(b)** Excess carrier lifetime vs excess carrier density for the stack/ZnO structure before and after (partial-area) sputtering of ITO, as well as 1 day and 9 days after sputtering. **(c)** Corresponding photoluminescence (PL) intensity imaging. The 2 × 2 cm^2 square region at the bottom corner of the sample was masked by quartz glass during the sputtering step. **(e)** Corresponding variation of τ_{eff} (effective carrier lifetime) and iV_{oc} (implied open-circuit voltage), with the J_0 (surface recombination current density prefactor) values provided in fA/cm^2.

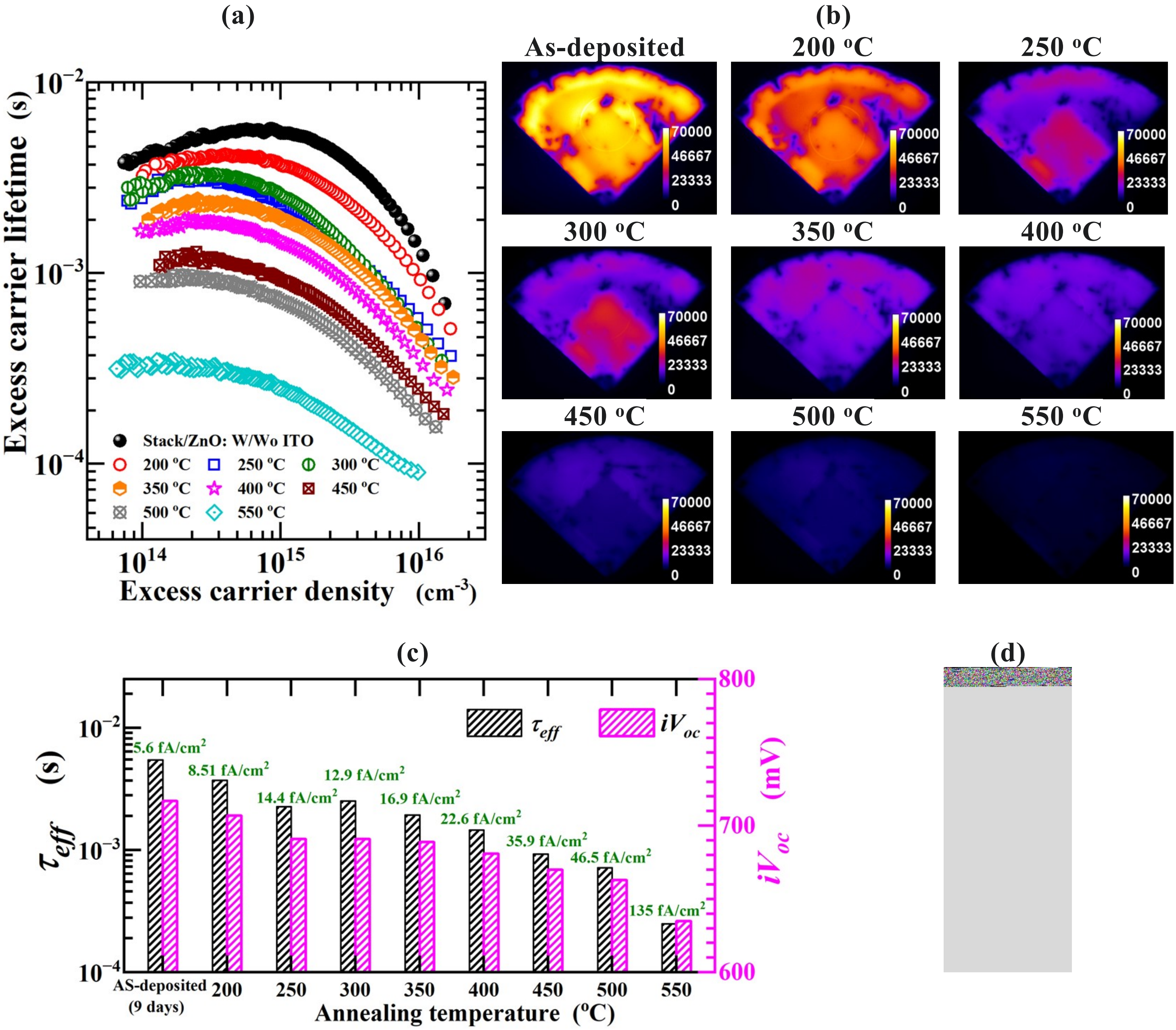

Figure S14 Excess carrier lifetime vs excess carrier density for the stack/ZnO structure, partially capped by ITO, of Figure S13, following annealing at a range of increasing temperatures in N_2 for 3 minutes per anneal. **(b)** Corresponding photoluminescence (PL) intensity imaging at each annealing temperature. **(c)** Corresponding variation of τ_{eff} (effective carrier lifetime) and iV_{oc} (implied open-circuit voltage) for these samples, with the J_0 (surface recombination current density prefactor) values provided in fA/cm^2. **(d)** Schematic diagram for the stack/ZnO structure with partial ITO coverage.

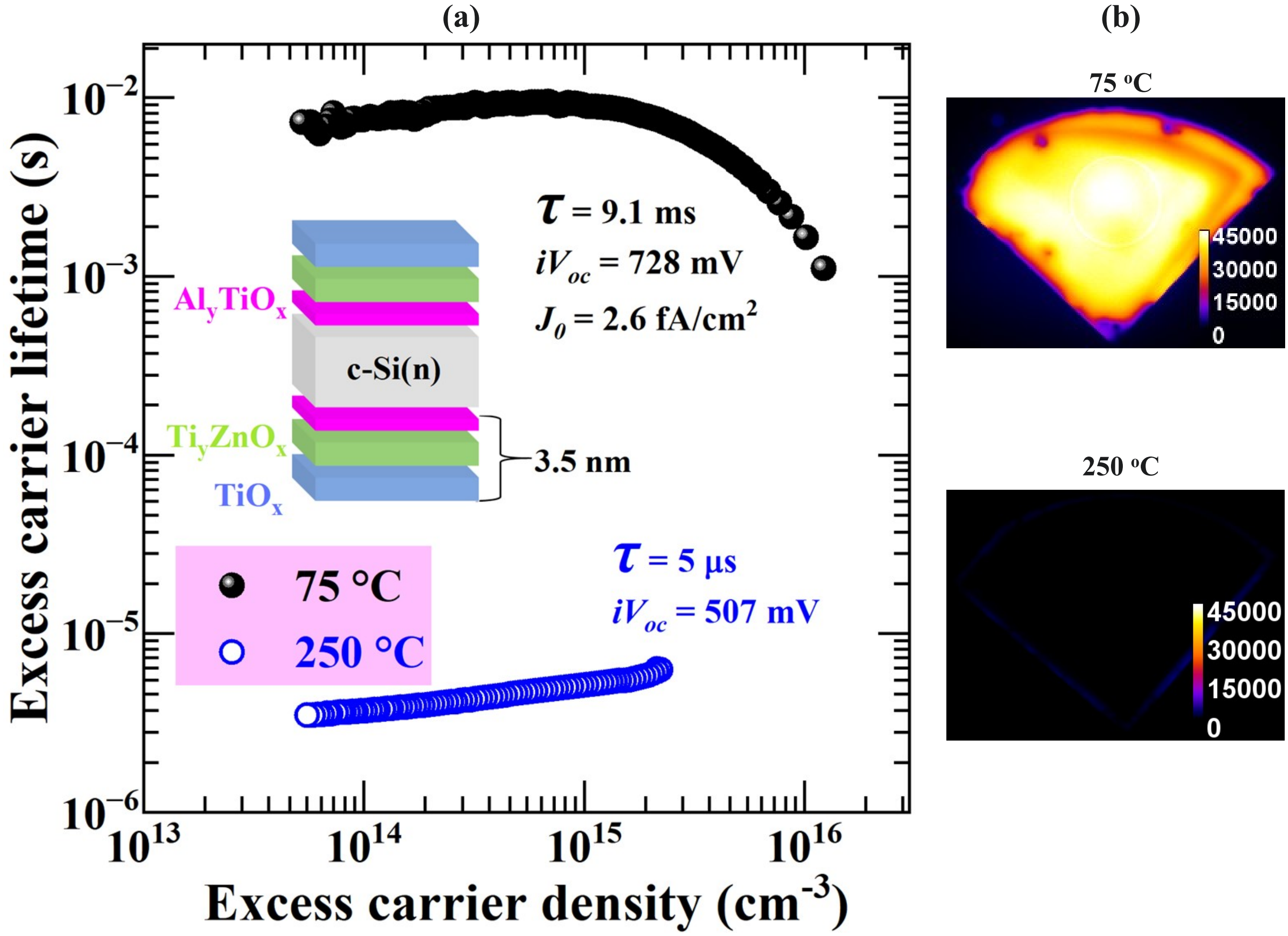

Figure S15(a) Excess carrier lifetime vs excess carrier density and **(b)** photoluminescence (PL) intensity images of lifetime test structures passivated by the $Al_yTiO_x/Ti_yZnO_x/TiO_x$ stack deposited at 75 °C and 200 °C. The inset shows a schematic diagram of the sample structure. The values of τ_{eff}, iV_{oc}, and J_0 at each deposition temperature are indicated.

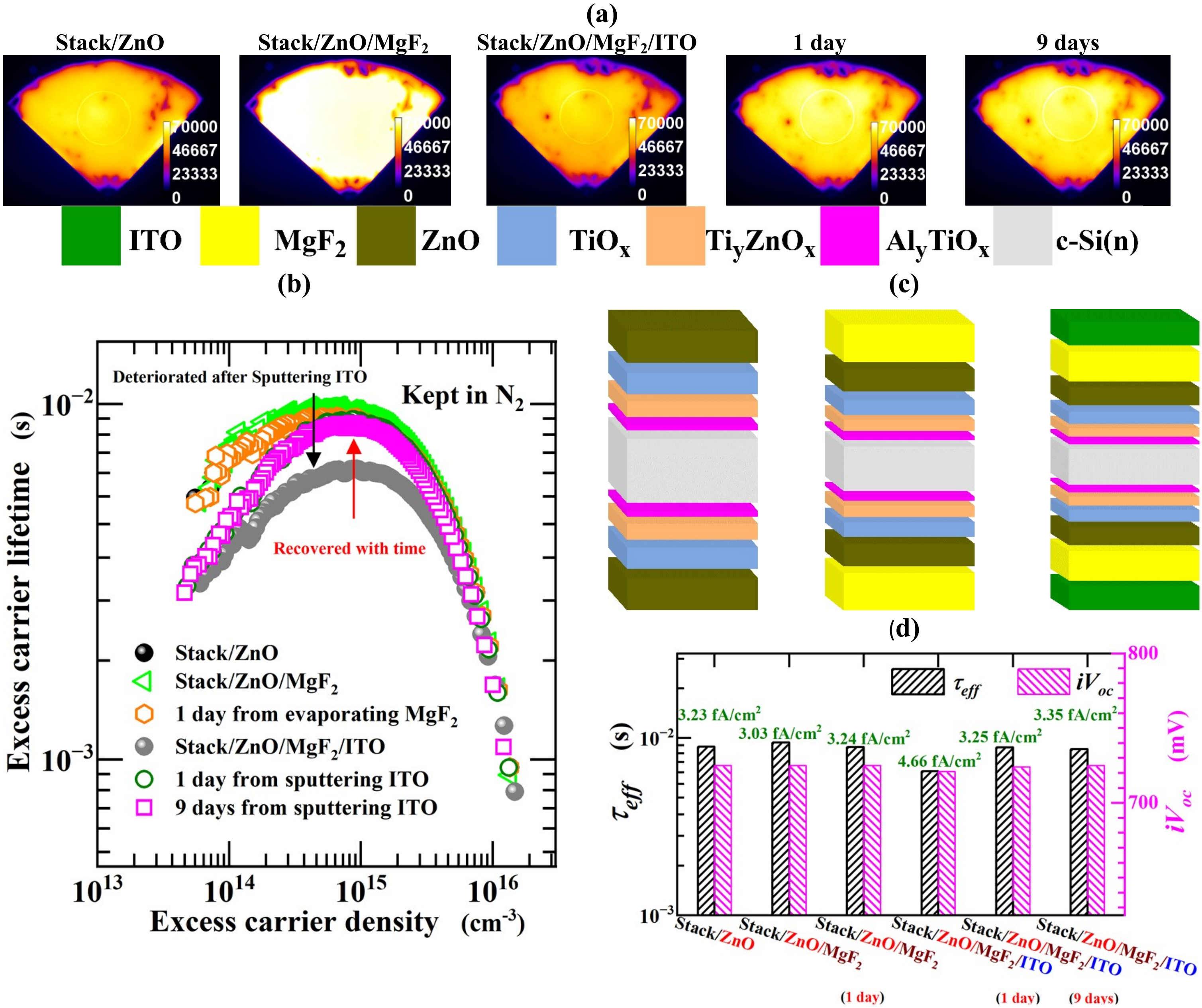

Figure S16 **(a)** Photoluminescence (PL) intensity imaging and **(b)** excess carrier lifetime vs excess carrier density for a lifetime test structure passivated by the $Al_yTiO_x/Ti_yZnO_x/TiO_x$ stack capped by ZnO: 1) before and 2) immediately after capping by MgF_2; 3) 1 day after capping by MgF_2; 4) immediately after subsequent sputtering of ITO; 5) 1 day after sputtering of ITO; and 6) 9 days after sputtering of ITO. **(c)** Schematic diagram of the stack/ZnO, stack/ZnO/MgF_2, and stack/ZnO/MgF_2/ITO sample structures. **(d)** Corresponding variation of τ_{eff} (effective carrier lifetime) and iV_{oc} (implied open-circuit voltage) for these samples, with the J_0 (surface recombination current density prefactor) values provided in fA/cm^2.

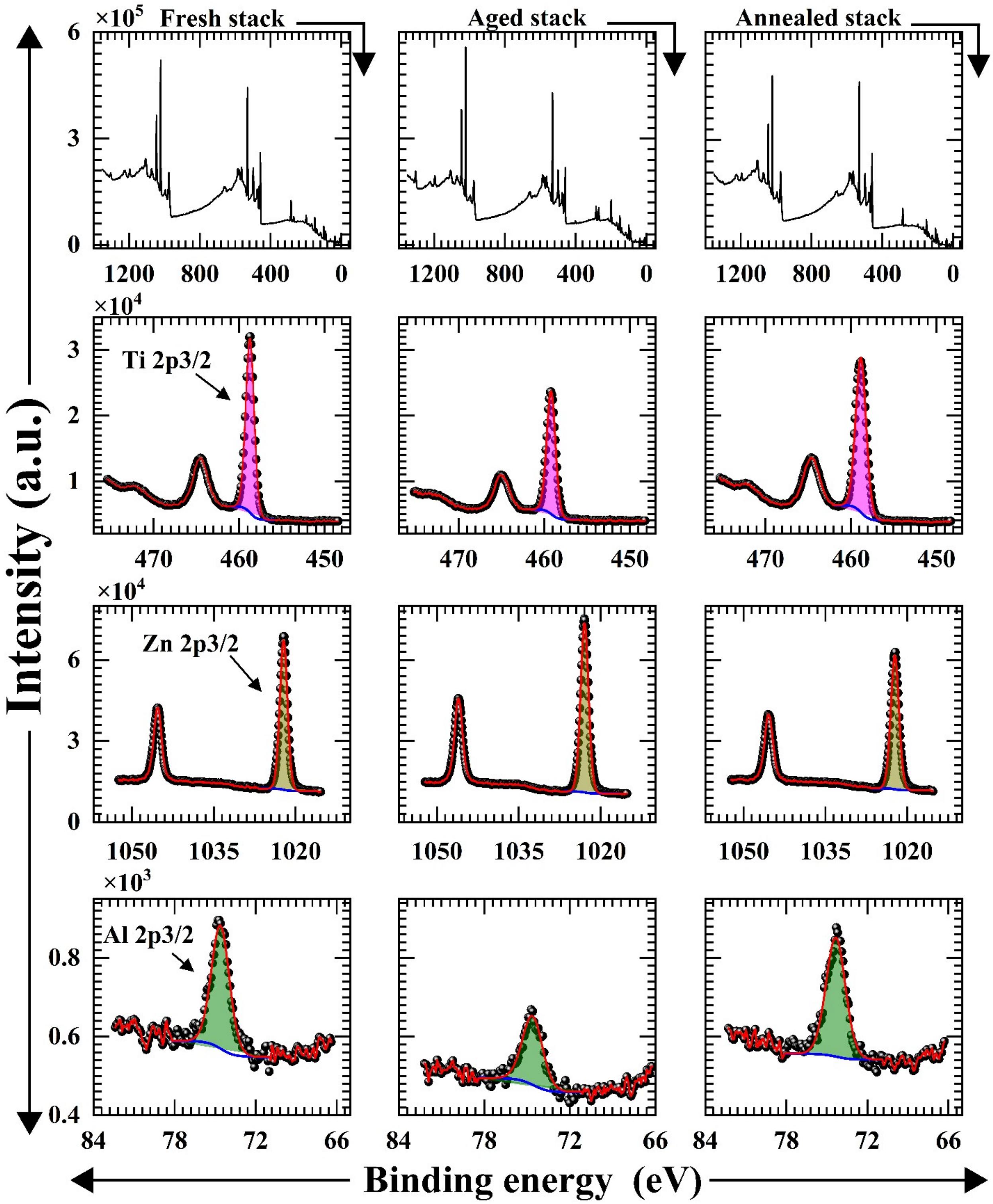

Figure S17 X-ray photoelectron spectroscopy (XPS) survey scan spectra and Ti 2p, Zn 2p, and Al 2p peak spectra, for the fresh $Al_yTiO_x/Ti_yZnO_x/TiO_x$ stack, the aged stack (measured after aging in air for 30 days), and the annealed stack (measured after annealing in N_2 for 3 minutes at 400 °C). Note that the fresh stack was measured on the fifth day after deposition and the annealed stack was measured on the fifth day after thermal treatment.

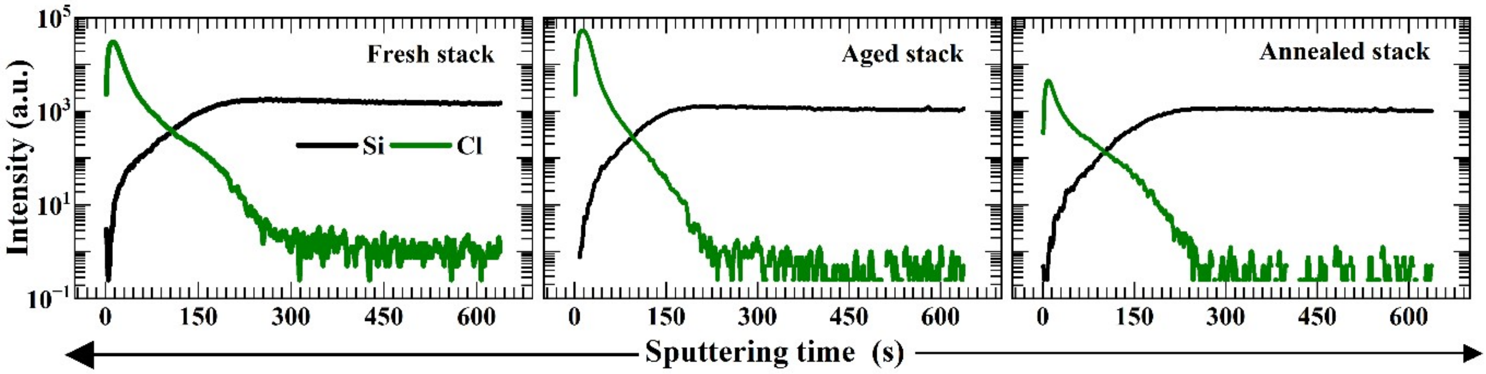

Figure S18 Secondary ion mass spectrometry (SIMS) depth profiles of Si and Cl, for the fresh $Al_yTiO_x/Ti_yZnO_x/TiO_x$ stack, the aged stack (measured after aging in air for 30 days), and the annealed stack (measured after annealing in N_2 for 3 minutes at 400 °C). Note that the fresh stack was measured on the fifth day after deposition and the annealed stack was measured on the fifth day after thermal treatment. The measurements were recorded under positive polarity by Bi_3^+.

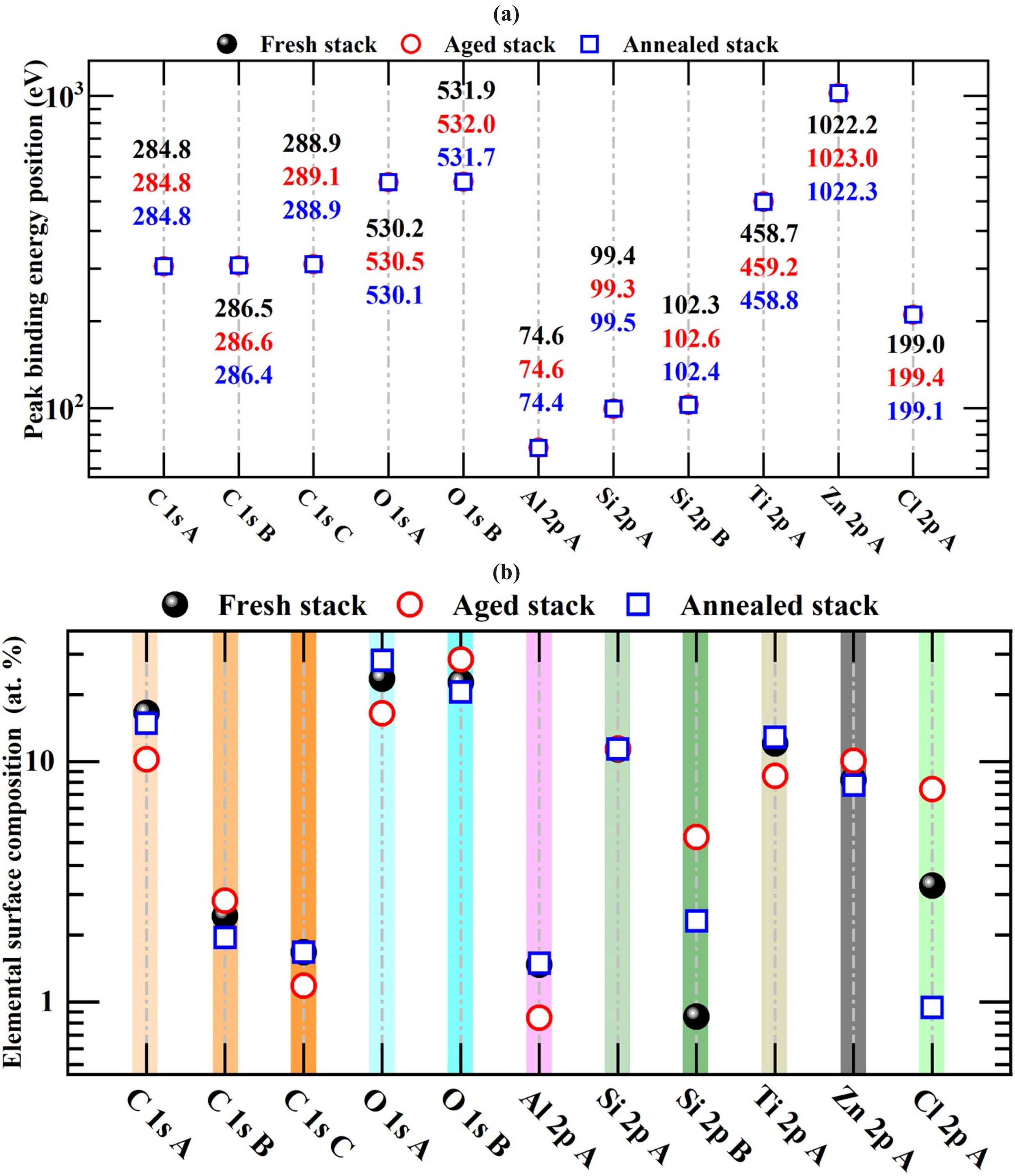

Figure S19 (a) Peak binding energy position and **(b)** atomic elemental surface composition for the fresh stack, the aged stack (measured after aging in air for 30 days), and the annealed stack (measured after annealing in N_2 for 3 minutes at 400 °C). Note that the fresh stack was measured on the fifth day after deposition and the annealed stack was measured on the fifth day after thermal treatment.

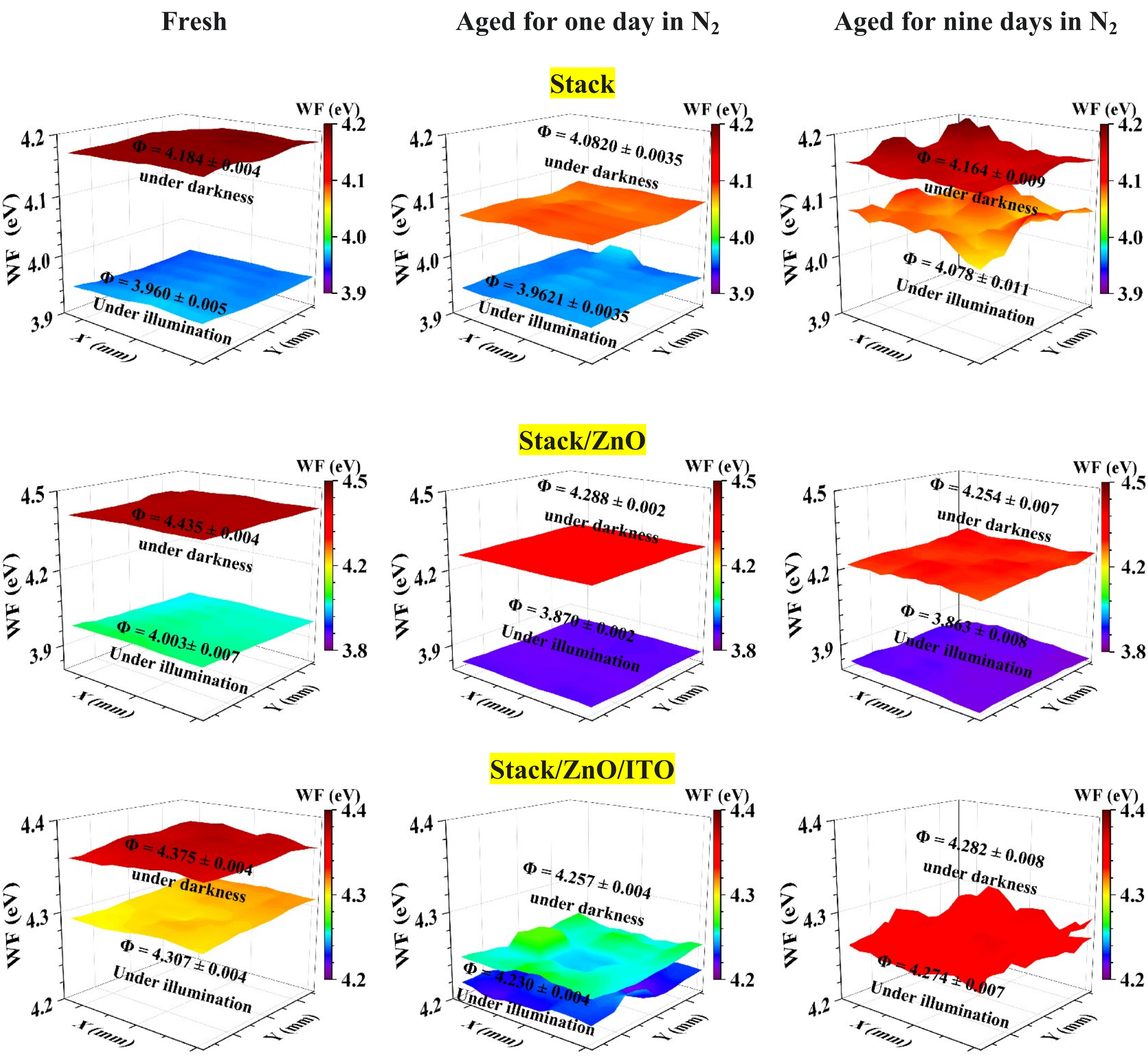

Figure S20 Work-function maps (2.4 mm × 2.25 mm) measured under darkness and illumination for the stack, stack/ZnO, or stack/ZnO/ITO configurations. The measurements were taken directly after deposition as well as at 1 day and 9 days after deposition.

(a)

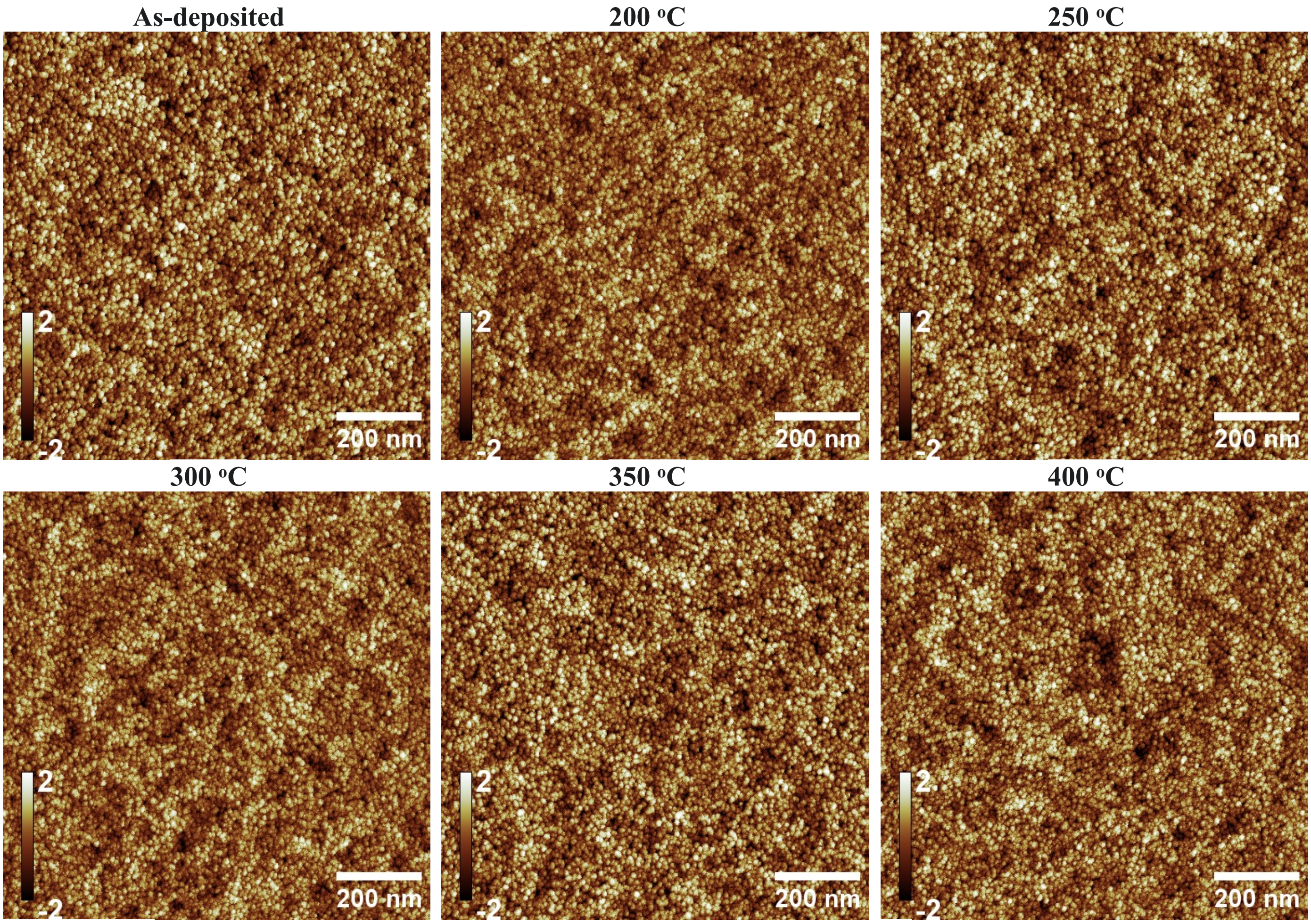

(b) (c)

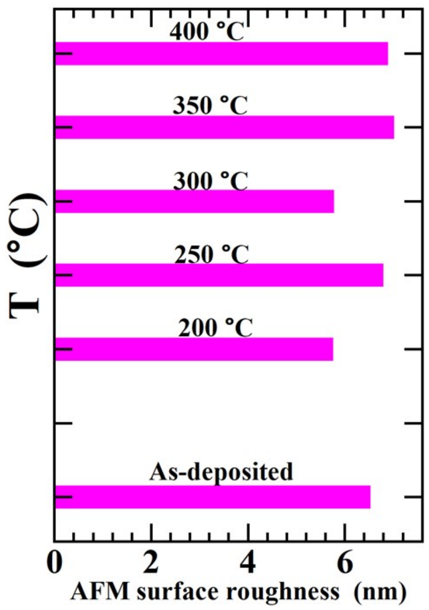

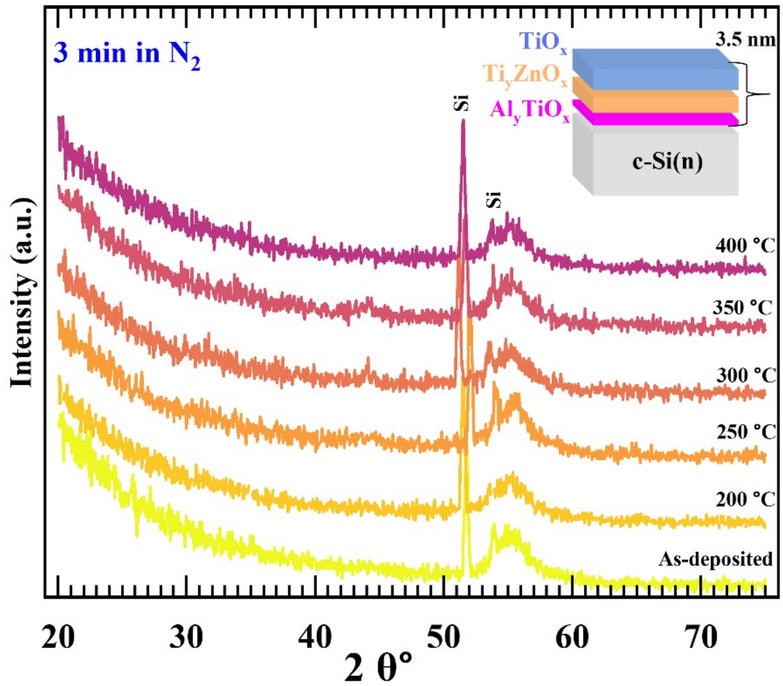

Figure S21 (a) AFM images, **(b)** RMS surface roughness, and **(c)** GIXRD spectra as a function of annealing temperature for the $Al_yTiO_x/Ti_yZnO_x/TiO_x$ stack on Si.

(a)

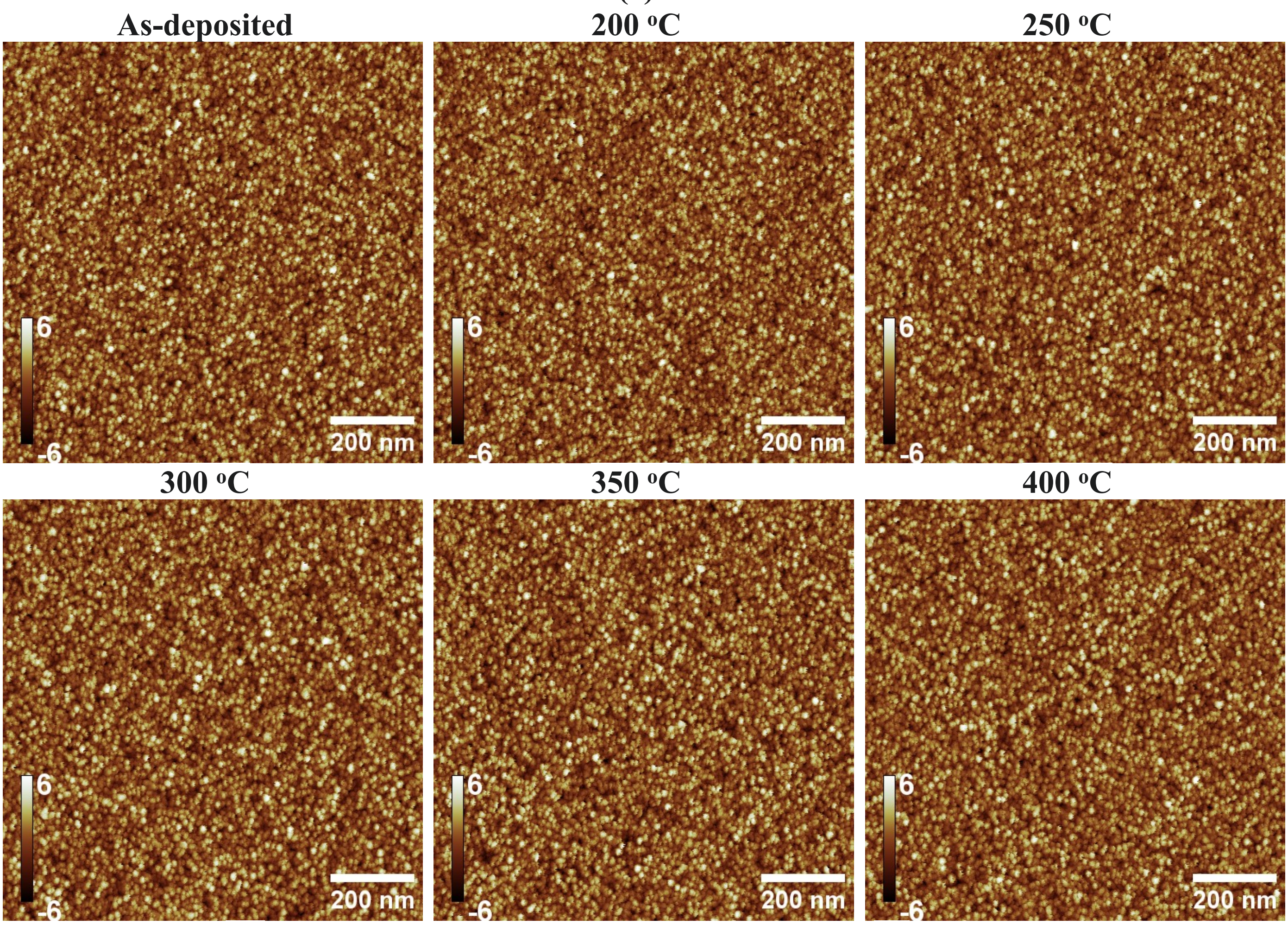

(b) **(c)**

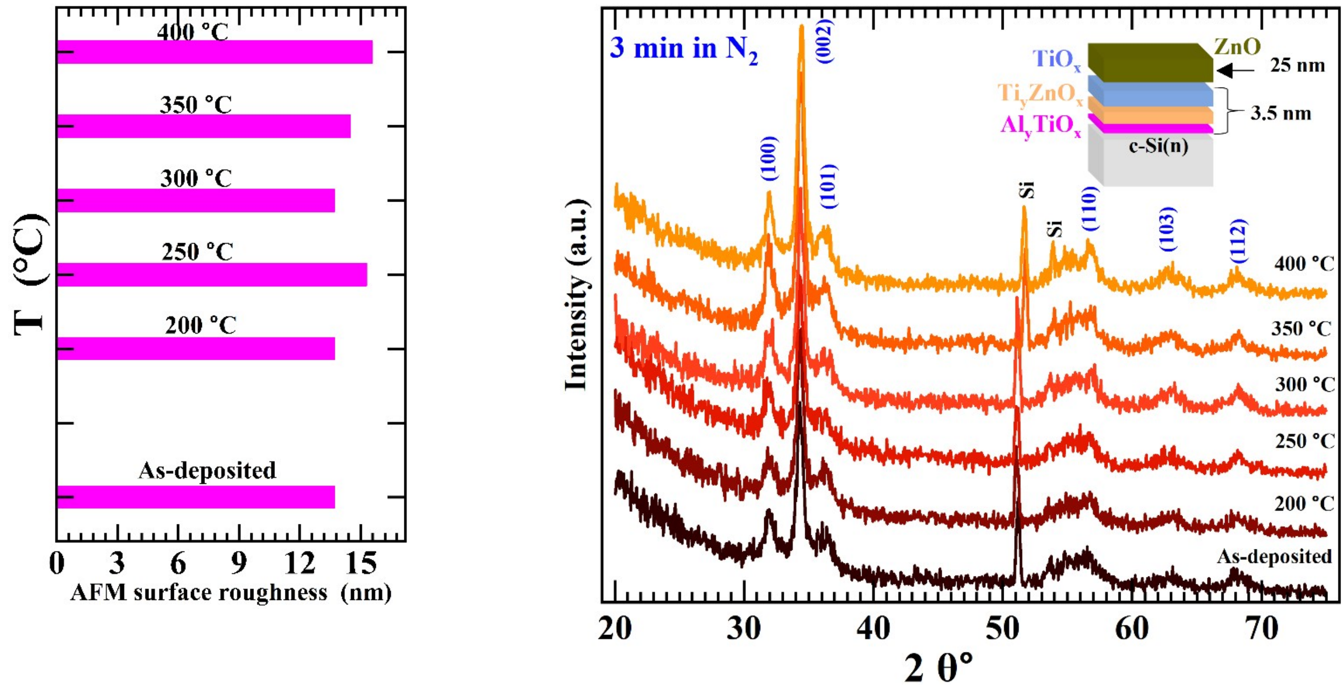

Figure S22 **(a)** AFM images, **(b)** RMS surface roughness, and **(c)** GIXRD spectra as a function of annealing temperature for the $Al_yTiO_x/Ti_yZnO_x/TiO_x$ stack capped by 25 nm of ZnO on Si.

(a)

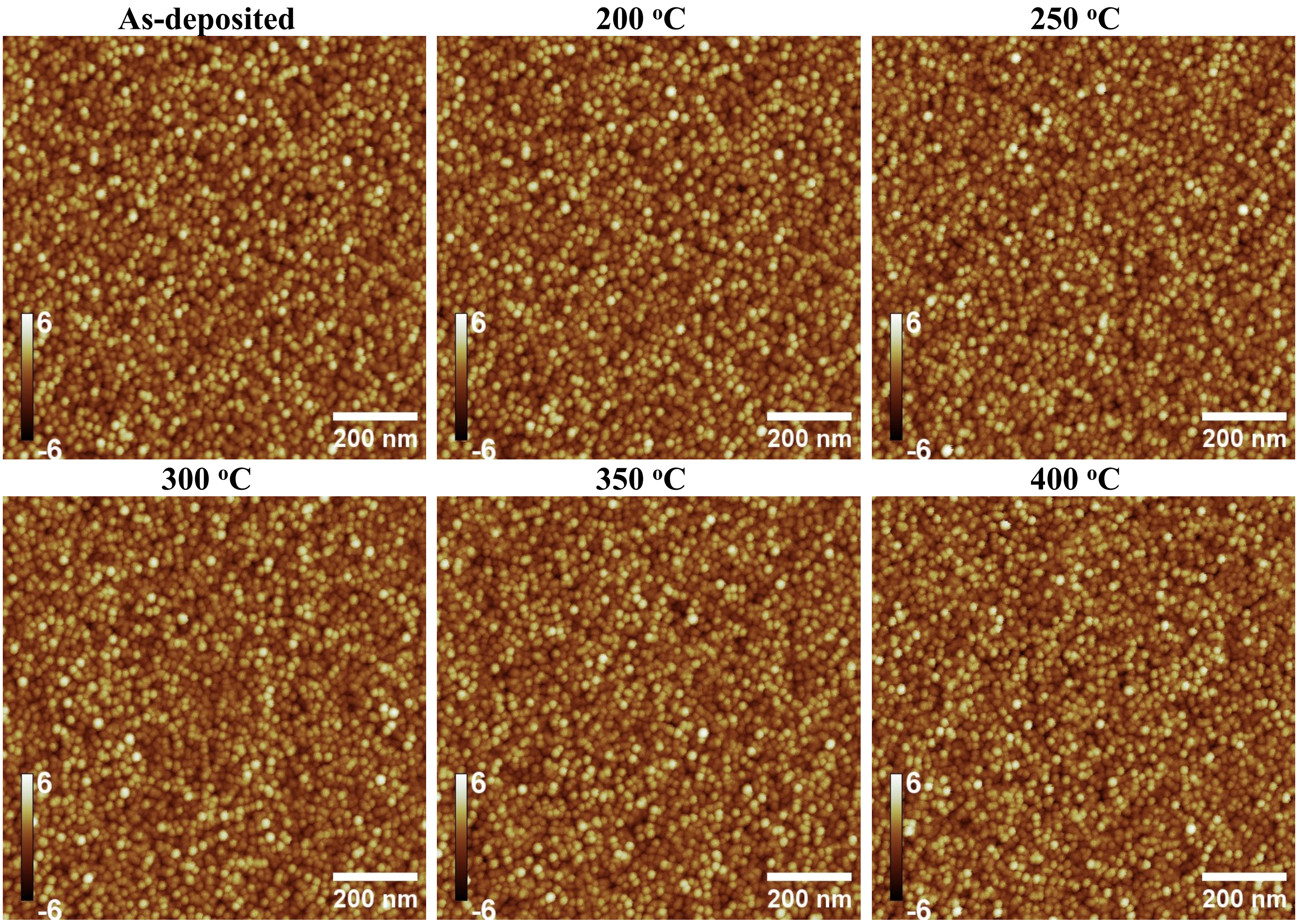

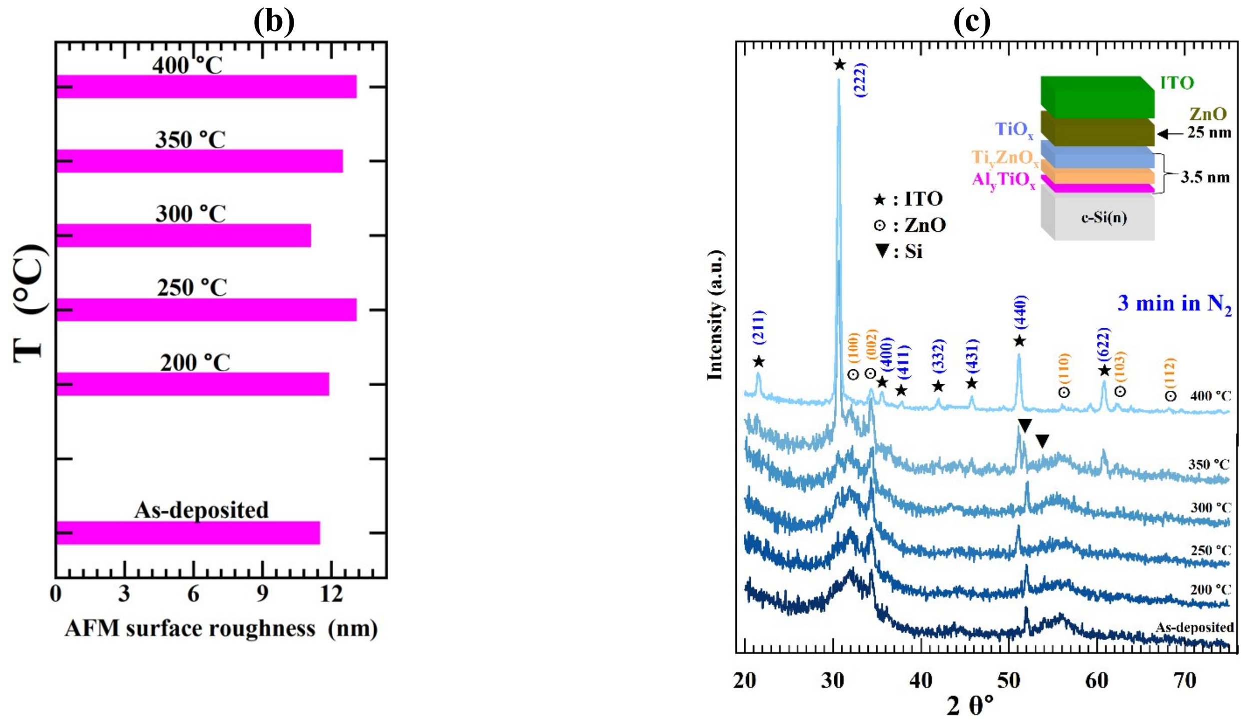

Figure S23 **(a)** AFM images, **(b)** RMS surface roughness, and **(c)** GIXRD spectra as a function of annealing temperature for the $Al_yTiO_x/Ti_yZnO_x/TiO_x$ stack capped by 25 nm of ZnO and 50 nm of ITO on Si.

Table S1 ALD process settings used for TiO_x, ZnO, and Al_2O_3 sub-cycles.

Deposited material	Precursor	Pulse (ms)	Purge (ms)
TiO_x	$TiCl_4$	50	750
	DI H_2O	50	750
ZnO	DEZ	50	2000

	DI H_2O	50	5000
Al_2O_3	TMA	50	750
	DI H_2O	50	750